Nuclear Instruments and Methods in Physics Research B 326 (2014) 293–297

Contents lists available at ScienceDirect

Nuclear Instruments and Methods in Physics Research B

journal homepage: www.elsevier.com/locate/nimb

Radiation stability test on multiphase glass ceramic and crystalline ceramic waste forms

Ming Tang [a,*], Anna Kossoy [a], Gordon Jarvinen [a], Jarrod Crum [b], Laura Turo [b], Brian Riley [b], Kyle Brinkman [c], Kevin Fox [c], Jake Amoroso [c], James Marra [c]

[a] Los Alamos National Laboratory, Los Alamos, NM 87545, USA
[b] Pacific Northwest National Laboratory, Richland, WA 99352, USA
[c] Savannah River National Laboratory, Aiken, SC 29808, USA

ARTICLE INFO

Article history:
Received 16 July 2013
Received in revised form 26 October 2013
Accepted 26 October 2013
Available online 3 February 2014

Keywords:
Glass ceramic
Crystalline ceramic
Waste form
Radiation damage
TEM

ABSTRACT

A radiation stability study was performed on glass ceramic and crystalline ceramic waste forms. These materials are candidate host materials for immobilizing alkali/alkaline earth (Cs/Sr-CS) + lanthanide (LN) + transition metal (TM) fission product waste streams from nuclear fuel reprocessing. In this study, glass ceramics were fabricated using a borosilicate glass as a matrix in which to incorporate CS/LN/TM combined waste streams. The major phases in these multiphase materials are powellite, oxyaptite, pollucite, celsian, and durable residual glass phases. Al_2O_3 and TiO_2 were combined with these waste components to produce multiphase crystalline ceramics containing hollandite-type phases, perovskites, pyrochlores and other minor metal titanate phases.

For the radiation stability test, selected glass ceramic and crystalline ceramic samples were exposed to different irradiation environments including low fluxes of high-energy (~1–5 MeV) protons and alpha particles generated by an ion accelerator, high fluxes of low-energy (hundreds of keV) krypton particles generated by an ion implanter, and *in-situ* electron irradiations in a transmission electron microscope. These irradiation experiments were performed to simulate self-radiation effects in a waste form. Ion irradiation-induced microstructural modifications were examined using X-ray diffraction and transmission electron microscopy. Our preliminary results reveal different radiation tolerance in different crystalline phases under various radiation damage environments. However, their stability may be rate dependent which may limit the waste loading that can be achieved.

1. Introduction

Exploration of options for reprocessing of used nuclear fuel remains of interest despite the current prevalence of a 'once-through' fuel cycle terminated by eventual geologic repository storage. A once-through fuel cycle means that the fuel experiences a single pass through a reactor after which it is packaged and becomes high-level waste (HLW), disposed of in a repository. Through the Fuel Cycle Research and Development (FCR&D) Program, the Department of Energy, Office of Nuclear Energy, is currently evaluating the modified-open nuclear fuel cycle to increase the efficiency of nuclear power production and reduce the amount of HLW. In the modified-open nuclear fuel cycle, the vast majority of the used fuel can be recycled, used for new fuel bundles, and sent back through a nuclear reactor. The envisioned fuel reprocessing technology would separate the fuel into several fractions, thus, partitioning the waste into groups with common chemistries. With these partitioned waste streams, it is possible to treat waste streams separately or combine waste streams for treatment when it is deemed appropriate. A portion of the fission products generated during burn up in a nuclear reactor are nonfissionable and, once separated from the fissionable material, must be immobilized in stable waste forms. The nonfissionable products targeted for an oxide waste form are in the following three waste streams generated with the projected transuranic extraction (TRUEX$^+$) process: alkalis/alkaline earths (CS representing ^{137}Cs and ^{90}Sr), lanthanides (LN), and transition metals (TM).

Multiphase borosilicate glass ceramics are one candidate waste form for immobilizing the combined CS+LN+TM-fission products [1,2]. Unlike borosilicate glass alone, which offers many favorable characteristics but suffers from low waste loading and potential issues stemming from low glass transition temperatures [3,4], glass-ceramic waste forms have the potential to provide both significantly higher waste loading and enhanced mechanical integrity due to the presence of crystalline phases [5]. The former benefit is

* Corresponding author. Tel.: +1 505 665 1472; fax: +1 505 667 8021.
E-mail address: mtang@lanl.gov (M. Tang).

0168-583X/$ - see front matter © 2014 Elsevier B.V. All rights reserved.
http://dx.doi.org/10.1016/j.nimb.2013.10.092

realized through designed crystalline phases grown during fabrication that immobilize elements that have low solubility in the glass phases. In the absence of such intentionally engineered phases, certain elements, most notably molybdenum and select lanthanides, will precipitate as various unwanted phases during the fabrication process or over time under storage and can appreciably degrade performance of the waste form [6–9].

Crystalline ceramic materials for HLW immobilization are another option [10–13]. Titanate ceramics have been thoroughly studied for use in immobilizing nuclear wastes (e.g., the SYNROC family) due to their natural resistance to leaching in water [11,12]. Assemblages of several titanate phases have been successfully demonstrated to incorporate radioactive waste elements, and the multiphase nature of these materials allows them to accommodate variation in the waste composition [13]. While these materials are typically densified via hot isostatic pressing, recent work has shown that they can also be produced from a melt process analogous to glass ceramic material processing. This production route is advantageous since melters are already in use for commercial and defense HLW vitrification in several countries, and melter technology greatly reduces the potential for airborne contamination as compared to powder handling operations.

The stability and durability of the vitrified waste forms need to be systematically investigated in order to assess their viability. This study focuses on radiation stability of waste forms made from both glass and crystalline phases. Most of the self-radiation in a waste form incorporating fission products is due to beta particle and gamma emission [14,15]. These emissions cause radiation damage primarily via radiolytic processes, because both beta and gamma particles induce substantial electronic excitations in a target material. Experimental techniques to examine radiation damage include: (1) Characterizing samples taken from reactors or other facilities (e.g., irradiated *in situ* by the full spectrum of radiation: neutron, α, β, and γ); (2) Characterizing samples irradiated by ion accelerator *ex situ*; (3) Irradiating samples in a transmission electron microscope (TEM) using high-energy electrons to simulate radiolysis effects; (4) Incorporating radionuclides into the material during processing whose radiation causes *in situ* or self-radiation.

Preliminary evaluations of the radiation stability of select glass ceramic and crystalline ceramic waste forms were undertaken by subjecting samples to ion irradiations at the Ion Beam Materials Lab (IBML), and *in-situ* electron irradiation in a TEM at the Electron Microscopy Lab (EML), Los Alamos National Laboratory (LANL). Light and heavy ion bombardment, and electron irradiations are used to simulate the self-radiation damage that occurs in a material incorporating nuclides undergoing radioactive decay. Light ions and electrons provide a useful means to examine radiolysis effects because they deposit nearly all of their energy in solids via electronic loss processes; heavy ions are used to simulate energetic recoil nuclei interaction which involves ballistic processes.

2. Experimental

The glass ceramic and crystalline ceramic waste forms were prepared at Pacific Northwest National Laboratory (PNNL) and Savannah River National Laboratory (SRNL) as reported previously [1,2,10]. The select samples were cut into pieces and polished with alumina lapping films (down to 1 μm) to obtain a mirror finish for further investigation. In preparation for ion irradiation, all samples were finally polished with a 40 nm colloidal silica slurry (Syton HT50, DuPont Air Products NanoMaterials L.L.C, Tempe, AZ), in order to remove the surface damage created by the previous mechanical polishing steps.

Ion irradiation experiments were performed at room temperature (~300 K) at IBML, using a 200 kV Danfysik high current research ion implanter and a 3.2 MeV Tandem accelerator. 600 keV Kr, 5 MeV alpha (He), and 2 MeV proton (H) beams were used in this study to evaluate radiation stability in these waste form materials. The Stopping and Range of Ions in Matter (SRIM) program [16] was used to estimate radiation dose in ion irradiated samples. A threshold displacement energy of 40 eV (this is an arbitrary assumption) was used for all target elements. Fig. 1 shows the results of this simulation for these compounds. The peak displacement damage dose for 600 keV Kr irradiation (Fig. 1(a)) is ~3.5 dpa at a fluence of 2.5×10^{19} Kr ions/m^2; the peak radiation dose for 5 MeV He irradiation $\sim 8 \times 10^9$ Gy at a fluence of 1×10^{21} He ions/m^2, and 8×10^9 Gy for 2 MeV H at a fluence of 4×10^{21} H ions/m^2 in Fig. 1(b).

For the *in-situ* electron beam irradiation study, a TEM specimen was prepared in plan-view geometry. This plan-view sample was

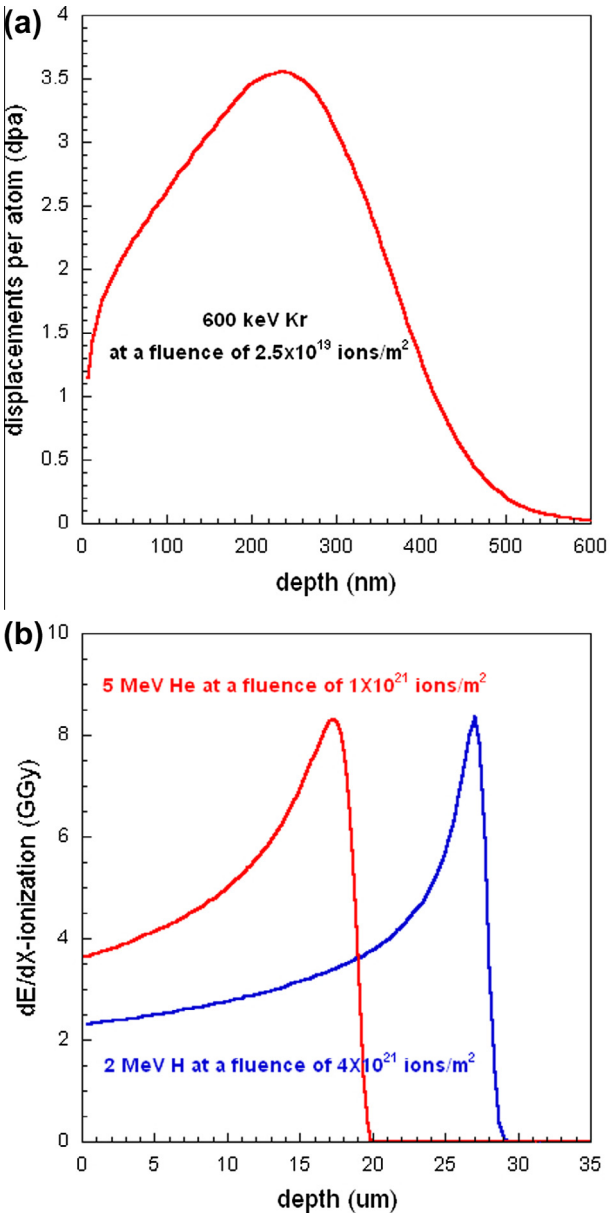

Fig. 1. (a) SRIM simulation results showing the radiation damage dose profile as a function of depth for 2 MeV H and 5 MeV He ion irradiation of a glass ceramic to a fluence of 4×10^{21} H/m^2, and 1×10^{21} He/m^2, respectively. (b) The displacement damage profile as a function of depth for 600 keV He ion irradiation of a glass ceramic to a fluence of 2.5×10^{19} Kr/m^2.

examined at room temperature in a FEI Tecnai F30 electron microscope operating at 300 kV. Electron irradiation experiments were carried out by focusing the electron beam onto small regions of electron transparent material (a typical irradiated region was ~100 nm diameter). During these *in-situ* electron beam irradiation experiments, the incident electron flux, measured using a faraday cup, was approximately 1.8×10^{24} e/m^2 s. Irradiations were performed over a range of fluences up to 1.08×10^{27} e/m^2 (corresponding to a radiation dose of 10^{13} Gy). Irradiations were performed with the electron beam aligned along high-index crystallographic directions. No crystal-orientation dependences of the structural changes described in this report were observed. Compared with the self-radiation dose rate (10^4–10^5 Gy/h) expected in Cs/Sr waste forms, the high dose rates of electron irradiation using electron microscopes (10^{11}–10^{13} Gy/h) and highly ionizing ion beams (such as protons or helium) using accelerators (10^7–10^8 Gy/h) offer the capability to study radiation effects over the ionizing dose range of interest on laboratory time scales. Available γ sources and doping with short-lived isotopes, such as ^{134}Cs, are not able to achieve the necessary dose level, due to the low dose rate or dopant level.

X-ray diffraction (XRD), scanning electron microscopy (SEM), and transmission electron microscopy (TEM) were used to characterize the phase composition and structural evolution in these waste forms. X-ray diffraction θ–2θ scans (Bragg-Brentano geometry) and grazing incidence (2θ) scans with an incidence angle of 1° were done on a Bruker AXS D8 Advanced X-ray diffractometer, using Cu-K_α radiation and a graphite monochromator. The XRD patterns collected for these glass ceramics and crystalline ceramics were quite complex because of the multiple phases present in the specimens and the high number of reflections in the patterns. SEM and Energy-Dispersive X-ray Spectroscopy (EDS) measurements were performed with a FEI Inspect SEM. These glass ceramic and crystalline ceramic samples were coated with 2 nm of carbon to prevent surface charging for SEM and TEM observations. Irradiated samples were also prepared in cross-sectional geometries for TEM examination. The ion irradiation-induced microstructure evolution was examined using a FEI Tecnai F30 electron microscope operating at 300 kV.

3. Results

The radiation stability of two glass ceramics with different waste streams and waste loadings, and one crystalline ceramic was tested under various radiation environments. Glass ceramic composition GC-4 includes the combined CS+LN waste streams with a waste loading of 60 mass%. Glass ceramic composition Mo-6.25 is formulated with the combined CS+LN+TM waste streams at a waste loading of 45 mass% in which 6.25 mass% is MoO_3 in the glass. Crystalline ceramic CSLNTM-2 incorporates CS+LN+TM high Mo (13.88 mass%) waste streams with a waste loading of 60 mass%.

3.1. Ion irradiation on multiphase glass ceramics

SEM micrographs in Fig. 2 show that the glass ceramics are highly crystallized with varying amounts of glass phase remaining. The SEM micrograph of GC-4 is shown in Fig. 2 (left). The crystalline phases in the GC-4 sample, which include lanthanide rich oxyapatite ($(Ca,Sr)_xNd_{(10-x)}Si_6O_{26}$), celsian ($(Ba,Sr)Al_2Si_2O_8$), pollucite ($CsAlSiO_6$), lanthanide borosilicate ($Ln_5BSi_2O_{13}$), and other minor phases, are determined by EDS, along with the XRD data. Boron cannot be detected with the EDS detector, so there is a possibility that boron is present in some or all of the phases. The remaining glass phase is a very small fraction that is confined to the grain boundaries and is not visible in this SEM micrograph. Fig. 2 (right) shows the SEM micrograph of glass ceramic Mo-6.25. The crystalline phases have been formed in various distinct crystal morphologies, and there is a remaining glass network that makes up the background or matrix of the images. The crystalline phases observed are similar to the GC-4 sample plus the addition of the Mo-powellite phase ($CaMoO_4$). The measured compositions for the powellite phase are drastically affected by the surrounding glass.

Glass ceramic sample GC-4 was subjected to a 5 MeV alpha (He-light ion) beam with a fluence of 1×10^{21} ions/m^2 (corresponding to a dose of 8×10^{10} Gy) and a 600 keV Kr (heavy ion) beam with a fluence of 2.5×10^{19} ions/m^2 (corresponding to a dose of 3.5 dpa) sequentially at room temperature to provide preliminary insight into the radiation damage tolerance of this glass ceramic waste form. The multiphase sample was evaluated by XRD before and after irradiation to identify any microstructural changes induced by ion irradiations (Fig. 3(a)). Under 5 MeV He irradiation, there are some differences in relative intensities among the peaks in the spectra but no changes in the phases present are apparent, indicating good radiation damage tolerance. The changes in relative intensity could be due to texturing since the spectra were collected from the polished surface of the sample, rather than crushed

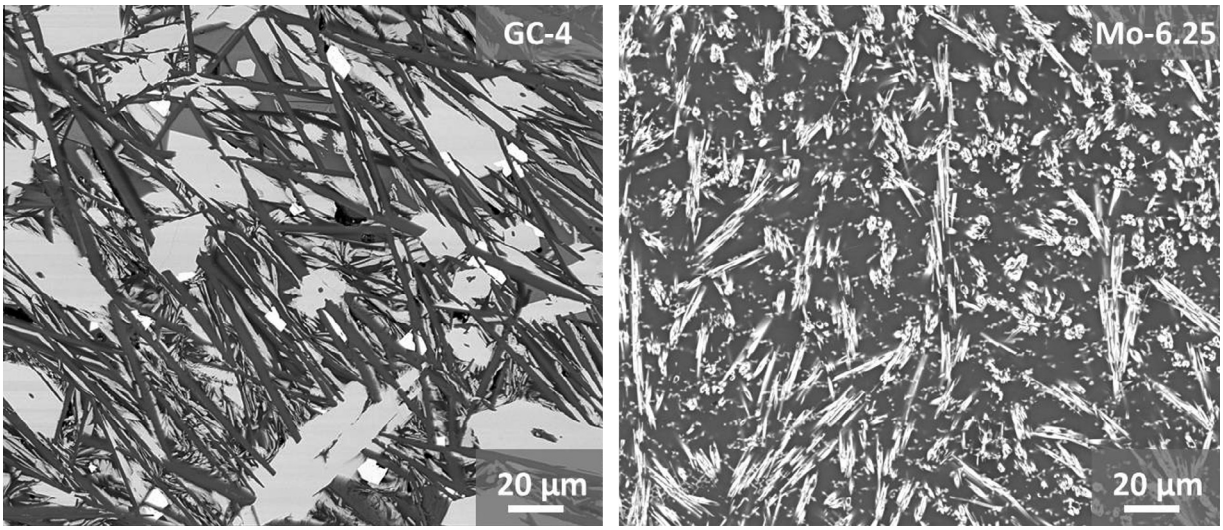

Fig. 2. Backscattered electron SEM micrographs of GC-4 (left) and Mo-6.25 glass ceramics.

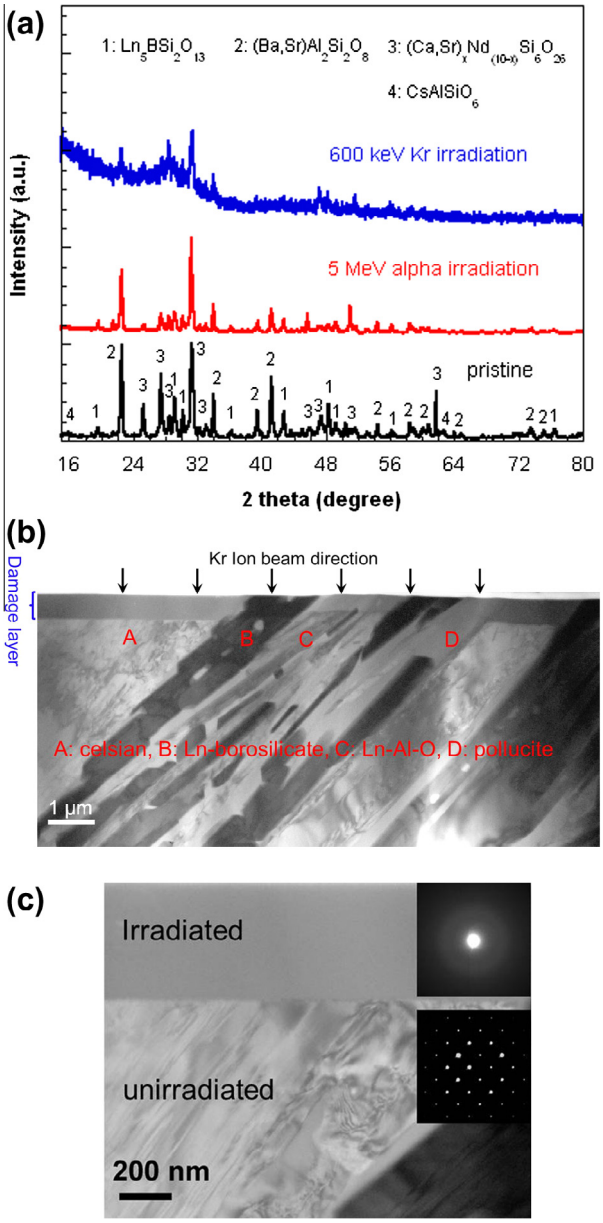

Fig. 3. (a) XRD results of GC-4 before and after He & Kr irradiations, (b) cross-sectional TEM micrograph of GC-4 irradiated with 600 keV Kr ions to a fluence of 2.5×10^{19} Kr/m^2 (~3.5 dpa), (c) bright-field image and inset SAED patterns of celsian phase in Kr irradiated GC-4 sample.

powders. Another possibility is that some crystalline structures have been recrystallized under irradiation. After 600 keV krypton irradiation, XRD measurement shows an apparent broad diffraction feature in the scattering angle $2\theta = 24–32°$, attributable to an amorphous structure. It indicates that a phase transformation from crystalline to amorphous occurs upon heavy ion irradiation.

Fig. 3(b) shows the result of cross-sectional TEM observation of Kr irradiated GC-4 sample. The micrograph reveals that the irradiation damage surface layer has thicknesses between 500 and 600 nm for this multiphase sample. Different thicknesses correspond to different crystalline phase compositions. Based on the EDS results under scanning transmission electron microscope (STEM) mode, four crystalline phase compositions including celsian, Ln-borosilicate, Ln–Al–O, and pollucite, are identified in the observed area. Electron diffraction studies indicate that these compositions possess their corresponding crystal structures. The differences in contrast in the damage layer suggest different microstructural evolution in different crystalline phases. In Fig. 3(c), the selected area electron diffraction (SAED) pattern from the unirradiated area can be indexed as corresponding to hexagonal cersian phase in a [0 1 1] orientation, and the diffuse halo in the SAED pattern corresponding to the damage layer indicates that Kr irradiation induces an amorphization in this celsian phase. A similar amorphous phase was observed in Ln–Al–O and Ln-borosilicate phases, while pollucite phase still remain crystalline under Kr irradiation (data not shown here). The above crystalline phases in multiphase waste form show the similar radiation response to the corresponding single phases under the similar radiation condition [17–19].

3.2. Ion irradiation on multiphase crystalline ceramics

A crystalline ceramic sample of composition CSLNTM-2 was analyzed using SEM/EDS. A backscattered electron micrograph of composition CSLNTM-2 is shown in Fig. 4(a). The differences in contrast in the SEM micrograph indicate at least four crystalline phases are present in this CSLNTM-2 sample with varying grain sizes and morphology. These four crystalline phases are identified using the results of EDS, which include Al_2O_3, powellite ($(Ca,Sr,Ba,Cd)MoO_4$), perovskite ($(Nd,Sm,Ce)TiO_3$), and zirconolite ($CaZrTi_2O_7$).

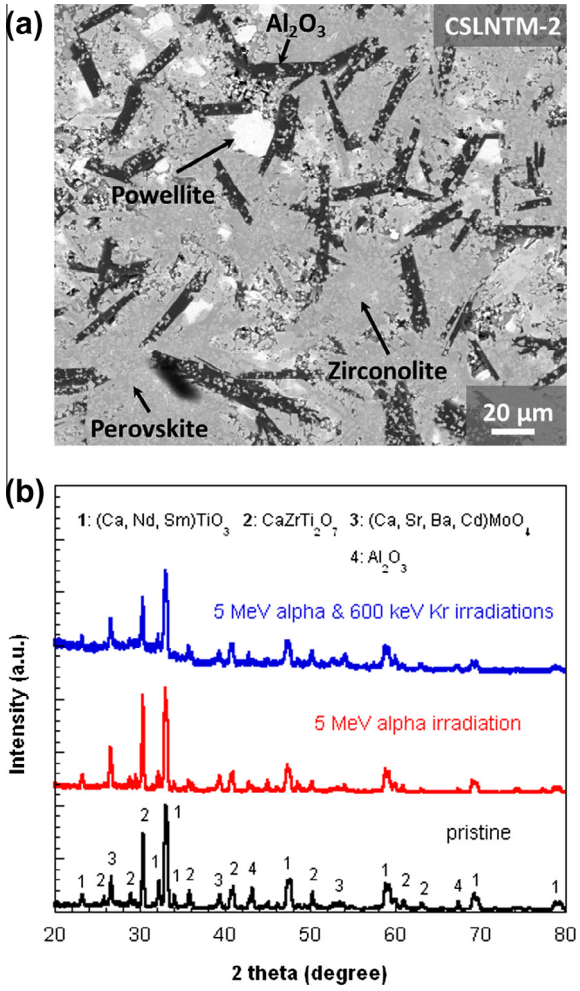

Fig. 4. (a) Backscattered electron SEM micrograph of CSLNTM-2 crystalline ceramic, (b) XRD results of CSLNTM-2 before and after He & Kr irradiations.

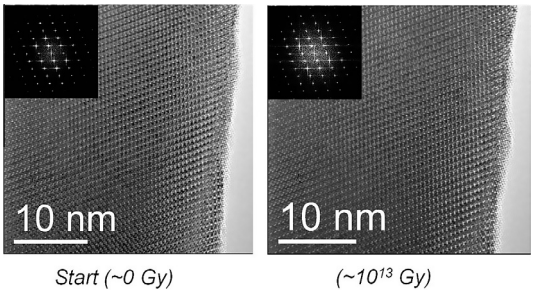

Fig. 5. High resolution transmission electron microscopy images including FFT diffractograms of oxyapatite phase in Mo-6.25 glass ceramic before (left) and after (right) electron irradiation to 10^{13} Gy.

Radiation stability of this multiphase crystalline ceramic waste form was tested under similar ion irradiations as glass ceramic sample GC-4. Fig. 4(b) shows XRD patterns obtained from a sample of crystalline ceramic CSLNTM-2 before and after light and heavy ion irradiations at room temperature; 5 MeV He ions with a fluence of 1×10^{21} ions/m^2 (corresponding to a dose of 8×10^{10} Gy) and 600 keV Kr (heavy ion) with a fluence of 2.5×10^{19} ions/m^2 (corresponding to a dose of 3.5 dpa) sequentially. Similar to the alpha irradiated GC-4 sample, there is little difference in the relative intensities among the peaks in the spectra between the pristine and He irradiated samples. However, after heavy ion Kr irradiation, the spectra changes significantly and an increased amorphous regime (near $2\theta = 26–34°$) appears after irradiation. The preliminary TEM studies (data not shown here) reveal that perovskite phase succumbs to radiation-induced amorphization, while Al_2O_3, powellite, and zirconolite phases still remain crystalline phases. The results agree with the radiation resistance of corresponding simple oxides in previous studies [20–22].

3.3. In-situ electron irradiation on certain crystalline phase in multiphase glass ceramic

Fig. 5 shows the results of the TEM/electron irradiation study for the oxyapatite phase ($Ca_2Ln_8Si_6O_{26}$) in glass ceramic Mo-6.25. An EDS spectrum under STEM mode was used to determine the oxyapatite phase composition (data not shown here). High resolution TEM images and inset fast Fourier transforms (FFT) indicate oxyapatite that maintains crystalline structure after a radiation dose of 10^{13} Gy (dose calculation using SRIM [16]). The results suggest that this oxyapatite phase exhibits stability to 1000 years at anticipated doses (2×10^{10}–2×10^{11} Gy) [15]. It is noted that actual self-radiation during waste form storage would come from β-particle fluxes that are orders of magnitude lower than those used in TEM irradiation experiments. Whether similar radiation damage and defect generation processes occur with low flux, long duration β-particle exposure as compared to high flux, short duration exposure to electrons in TEM experiments requires careful studies and is the subject of substantial current efforts.

4. Conclusion

Radiation stability on multiphase glass ceramic and crystalline ceramic waste forms has been investigated upon 2 MeV H, 5 MeV He, 600 keV Kr ion irradiations, and *in-situ* electron irradiation in TEM at room temperature. These ion beam irradiation results indicate that these materials are radiation tolerant to the β-particles and γ-rays, but susceptible to amorphization under recoil nuclei effects. *In-situ* electron irradiation results indicate that the oxyapatite phase retains its crystalline structure after a radiation dose of 10^{13} Gy, which is equivalent to roughly 1000 y of self-irradiation dose for a highly loaded Cs/Sr waste form [15]. Overall, different crystalline phases in these multiphase waste forms exhibit different radiation tolerance under various radiation damage environments. Further experiments are now in progress to explore radiation tolerance of these crystalline phases in multiphase waste forms and compare with that of the corresponding single phase in more detail.

Acknowledgements

The authors would like to thank the Department of Energy Office of Nuclear Energy (DOE-NE) for funding this work under the Fuel Cycle Research and Development Program. The authors would also like to thank J. Vienna (Pacific Northwest National Laboratory), T. Todd (Idaho National Laboratory), and J. Bresee (DOE-NE) for project oversight and guidance.

References

[1] J. Crum, L. Turo, B. Riley, M. Tang, A. Kossoy-Simakov, J. Am. Ceram. Soc. 95 (2012) 1297–1303.
[2] J.V. Crum, A.L. Billings, J.B. Lang, J.C. Marra, C.P. Rodriguez, J.V. Ryan, J.D. Vienna, Baseline Glass Development for Combined Fission Products Waste Streams, AFCI-WAST-WAST-MI-DV-2009-000075, Pacific Northwest National Laboratory, Richland, WA, 2009.
[3] J.C. Cunnane, J.K. Bates, W.L. Ebert, X. Feng, J.J. Mazer, D.J. Wronkiewicz, J. Sproull, W.L. Bourcier, B.P. McGrail, MRS Res. Soc. Symp. Proc. 294 (1993) 225–232.
[4] M.J. Plodinec, Glass Technol. 41 (6) (2000) 186–192.
[5] T. Taurines, B. Boizot, J. Am. Ceram. Soc. 95 (3) (2012) 1101–1111.
[6] D.S. Kim, D.K. Peeler, P. Hrma, in: V. Jain, R. Palmer (Eds.), Proceedings of the Ceramic Transactions: Environmental Issues and Waste Management Technologies in the Ceramic and Nuclear Industries, 61, The American Ceramics Society, Westerville, OH, (1995) 177–185.
[7] B.J. Riley, P.R. Hrma, J. Rosario, J.D. Vienna, in: G.L. Smith, S.K. Sundaram, D.R. Spearing (Eds.), Proceedings of the Ceramic Transactions: Environmental Issues and Waste Management Technologies in the Ceramic and Nuclear Industries VII, 132, The American Ceramic Society, Westerville, OH, (2002) 257–265.
[8] A. Kossoy, R. Schulze, M. Tang, D.J. Safarik, R.J. McCabe, J. Nucl. Mater. 437 (2013) 216.
[9] K.S. Brinkman, K.M. Fox, J.C. Marra, J. Reppert, J.V. Crum, M. Tang, J. Alloys Compd. 551 (2013) 136.
[10] A.L. Billings, K.S. Brinkman, K.M. Fox, J.C. Marra, M. Tang, K.E. Sickafus, Adv. Mater. Sci. Environ. Nucl. Technol. II 227 (2011), http://dx.doi.org/10.1002/9781118144527.ch18.
[11] A.E. Ringwood, E.S. Kesson, N.G. Ware, W. Hibberson, A. Major, Nature 278 (1979) 219.
[12] A.E. Ringwood, E.S. Kesson, K.D. Reeve, D.M. Levins, E.J. Ramm, in: W. Lutze, R.C. Ewing (Eds.), Radioactive Waste Forms for the Future, Elsevier, North-Holland, Amsterdam, Netherlands, 1988, pp. 233–334.
[13] D.S. Perera, B.D. Begg, E.R. Vance, M.W.A. Stewart, Adv. Technol. Mater. Mater. Process. 6 (2) (2004) 214–217.
[14] W.J. Weber, R.C. Ewing, C.R.A. Catlow, T. Diaz de la Rubia, L.W. Hobbs, C. Kinoshita, Hj. Matzke, A.T. Motta, M. Nastasi, E.K.H. Salje, E.R. Vance, S.J. Zinkle, J. Mater. Res. 13 (1998) 1434.
[15] W.J. Weber, A. Navrotsky, S. Stefanovsky, E.R. Vance, E. Vernaz, MRS Bull. 34 (2009) 46–53.
[16] J.F. Ziegler, J.P. Biersack, U. Littmark, The Stopping and Range of Ions in Solids, Pergamon Press, New York, 1985.
[17] J. Fortner, S. Aase, D. Reed, Mater. Res. Soc. Symp. Proc. 713 (2002) 527.
[18] W.J. Weber, Y. Zhang, H. Xiao, L. Wang, RSC Adv. 2 (2012) 595.
[19] A. Meldrum, L.M. Wang, R.C. Ewing, Am. Mineral. 82 (1997) 858.
[20] R. Devanathan, W.J. Weber, K.E. Sickafus, M. Nastasi, L.M. Wang, S.X. Wang, Nucl. Instr. Meth. B 141 (1998) 366.
[21] Y. Zhang, J. Lian, C.M. Wang, W. Jiang, R.C. Ewing, W.J. Weber, Phys. Rev. B 72 (2005) 094112.
[22] M. Tang, P. Fuierer, P. Dickens, E. Fu, Phys. Status Solidi C 10–2 (2013) 216.